XLVI CILAMCE
VITÓRIA - ES - BRAZIL - 2025
XLVI IBERO-LATIN AMERICAN CONGRESS ON COMPUTATIONAL METHODS IN ENGINEERING

Mechanical Characterization and Finite Element Modeling of the Orthotropic Behavior of Woven Fabrics

Dante A. C. Gonçalves[1], Gabriel Fornazaro[1], Jelder Q. Velasquez[1], Felipe B. De Souza[1]

[1] *SENAI Institute of Innovation in Structural Engineering (ISI-EE)*
361 José Correa de Aguiar Street, Jardim Leblon, 87053-276, Maringá/Paraná, Brazil.
dante.goncalves@sistemafiep.org.br, gabriel.fornazaro@sistemafiep.org.br,
jelder.velasquez@sistemafiep.org.br, felipe.souza@sistemafiep.org.br

Abstract. Woven technical fabrics have been increasingly used as components in the automotive, aerospace, and biomedical sectors due to their high strength-to-weight ratio and flexibility. Polyester fabrics with plain and twill weave architectures exhibit orthotropic mechanical properties resulting from the yarn orientation in warp and weft directions. This study investigates experimentally and numerically the elastic behavior of a polyester fabric with a 2x2 twill weave. Uniaxial tensile tests were conducted at 0°, 45°, and 90° following ISO 13934-1, which defines the strip method for determining maximum force and elongation at break. The results confirmed orthotropic behavior, with varying stiffness and strength among directions. Numerical simulations were performed in Radioss using the LAW58 model, with membrane elements to represent the fabric. A methodology is proposed to characterize the fabric's in-plane response in the three directions without requiring experimental shear tests. The approach allows for accurate reproduction of the diagonal response using only axial test data. The proposed framework supports further studies involving multiaxial loading, forming processes, or integration into layered composites. This work contributes to computational modeling of orthotropic materials and offers a validated method for simulating synthetic woven fabrics in engineering applications.

Keywords: Finite element modeling, Woven textiles, Orthotropic behavior, Material characterization.

1 Introduction

Woven technical fabrics have been widely employed in structural applications in the automotive, aerospace, and civil engineering sectors, primarily due to their high strength-to-weight ratio and flexibility as discussed by Hosseini *et al.* [1] and by Kashani and Milani [2]. This material exhibits orthotropy that stems from the orientation of the yarns in the warp and weft directions, as well as from the interlacing architecture, such as plain, twill, or satin weaves. The fundamental structure of woven fabrics consists of the orthogonal interlacing of two yarn systems: warp yarns, aligned in the longitudinal direction, and weft yarns, aligned in the transverse direction. This geometric arrangement is schematically illustrated in Fig. 1, showing the right-angle intersection between the two yarn systems that define the fabric's architecture, as described by Das Neves et al. [3].

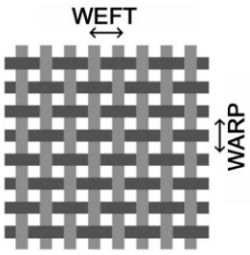


Figure 1 – Warp and weft representation. Retrieved from: DAS NEVES, Érica Pereira et al. (2020).

This interlacing geometry directly influences the mechanical behavior of fabrics, especially their stiffness and strength under loads applied in different directions. The mechanical characterization of such materials, which is essential for their use in computational simulations and structural design, is traditionally performed through uniaxial tensile tests. Tests conducted in the 0°, 90°, and 45° directions allow the determination of the main elastic properties and the evaluation of the material's orthotropic response. The response at 45° is strongly related to in-plane shear stiffness and is frequently used as a validation criterion for constitutive models, as emphasized by Gao and Wang [4]. The use of membrane elements in finite element software enables accurate simulation of the in-plane fabric behavior, provided that orthotropic properties are properly defined from experimental data.

Bydełek *et al.* [5] conducted a numerical modeling study of woven fabrics in Abaqus/Explicit using the FABRIC material model. In their work, experimental data, boundary conditions, and loading configurations were defined for four different fabrics, following the guidelines in the Abaqus User's Manual (2014), version 6.14 [6], specifically Section 23.4.1, which details the FABRIC formulation for characterizing fabric materials. Their approach included the definition of orthotropic behavior and the appropriate finite element selection. The shear response was determined using the picture-frame shear test, as illustrated in Fig. 2, which enables controlled in-plane shear deformation by displacing the frame, allowing accurate extraction of the shear stress–shear angle relationship.

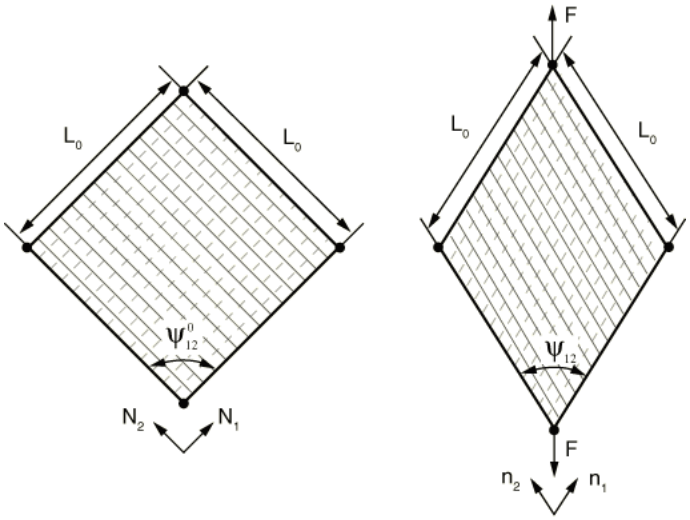


Figure 2 – Picture-frame shear test on a fabric. Retrieved from: Abaqus User's Manual (2014).

In this context, the present work proposes an integrated experimental and numerical methodology for characterizing the orthotropic behavior of woven fabrics, based on uniaxial tensile tests in multiple directions and subsequent finite element modeling.

2 Methodology

2.1 Experimental Methodology

Tensile tests of the Kairo Noir fabric, a 2x2 batavia weave, were performed according to ISO 13934-1 [7], which specifies the strip method for determining the tensile properties of textile fabrics. The specimens were flat rectangular samples measuring 280 mm in length, 50 mm in width, and an average thickness of 0.587 mm. The gauge length was set to 200 mm. Tests were conducted using an Instron universal testing machine, model 5900R 4467, under displacement control with a constant crosshead speed of 100 mm/min. For each principal fabric orientation, warp (0°), weft (90°), and bias (45°), five tests were performed, totaling fifteen specimens. Tensile stress was calculated as the ratio of the measured force to the cross-sectional area, while strain was computed based on the relative displacement of the specimen with respect to its initial length.

2.2 Numerical Methodology

Subsequently, following the approach of Bydełek *et al.* [4], an alternative numerical model and simulation environment using Radioss with the LAW58_FABR_A formulation was employed to characterize the Kario Noir fabric. The validation procedure, based on the 45° shear response, was maintained to ensure both consistency and physical representativeness of the material behavior under different loading conditions. Numerical modeling of the tensile tests was performed using HyperMesh for mesh generation and input definition, with the analyses executed in the Radioss solver. The geometry was defined according to the dimensions of the specimens tested experimentally, three rectangular specimens were modeled, with principal fiber orientations of 0°, 45°, and 90° relative to the local coordinate system.

First-order (linear) quadrilateral shell elements with a 2 mm side length were adopted to balance mesh resolution and computational efficiency. To simulate the effect of the testing machine grips, rigid regions were created at the top and bottom ends of the specimens, connected to reference points (rigid bodies) via coupling elements. The lower reference points were fixed, while the upper ones were subjected to a prescribed displacement at a constant speed of 100 mm/min, replicating the experimental test conditions. The simulation model is illustrated in Fig. 3. The material used in the simulations was LAW58_FABR_A, which allows modeling of orthotropic fabrics with nonlinear behavior. Property /PROP/TYPE16 (SH_FABR) was applied, with a thickness of 0.587 mm, initial fiber orientation of 0°, and an angular spacing of 90° between the principal directions.

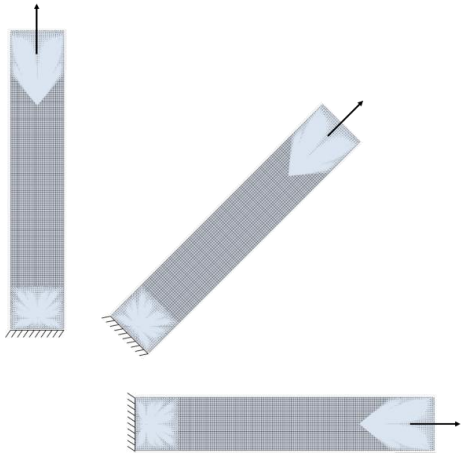


Figure 3 – Specimen Configuration and Boundary Conditions in HyperMesh.

The material model was defined according to the Radioss Help (2021) [8], which provides a detailed formulation for the use of LAW58 in fabric simulations. The interpretation of this formulation and its governing equations was fundamental for defining the material properties, as understanding the role and physical meaning of each parameter enabled the selection of those to be included in the model and allowed the estimation of initial values directly from the experimental data. The LAW58 material model allows for input either through direct experimental data from biaxial and shear test curves or by specifying material parameters corresponding to the three principal directions: warp (direction 1), weft (direction 2), and in-plane shear (12), simultaneously. This flexibility enables accurate representation of the fabric's orthotropic behavior based on the available characterization data. The main parameters used in the material definition are:

E_1: Young's modulus in the warp direction;
E_2: Young's modulus in the weft direction;
G_0: Initial shear modulus;
G_T: Tangent shear modulus at the shear locking angle α_T;
α_T: Shear locking angle;
S_1: Straightening strain in the warp direction;
S_2: Straightening strain in the weft direction;

$Flex_1$: Fiber bending modulus reduction factor in the warp direction;
$Flex_2$: Fiber bending modulus reduction factor in the weft direction.

These parameters and their physical interpretation are illustrated in Fig. 4, which schematically represents the nonlinear orthotropic behavior captured by the LAW58_FABR_A model. The left graph shows the tensile response, highlighting the straightening strain, the initial modulus and the transition to the full fiber stiffness. The right graph represents the shear behavior as a function of the shear angle, including the initial shear modulus, the shear locking angle, and the tangent modulus that governs the post-locking regime.

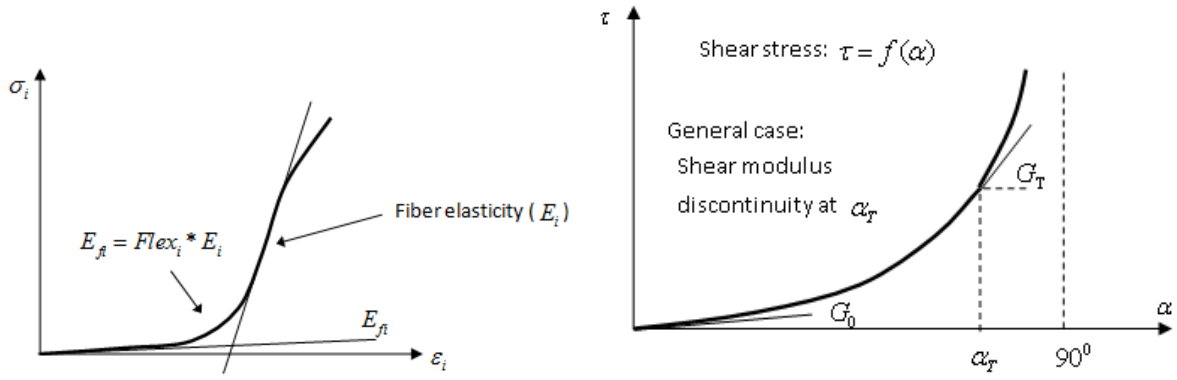


Figure 4 – Nonlinear orthotropic behavior of woven fabrics in the LAW58_FABR_A model. Retrieved from: Altair Engineering Inc. Radioss Help (2021).

The fiber elastic modulus in the final phase of loading can be determined from the slope of the stress–strain curve in this region. The initial straightening phase of the material response is described by eq. (1), which relates the fiber modulus to the initial modulus through the scaling factor $Flex_i$. The shear behavior is represented in two distinct stages: before and after the shear lock angle α_T, as given by eq. (2) and eq. (3), respectively. The post-lock shear modulus incorporates the initial shear response through the auxiliary term G_A, defined in eq. (4). At any deformation stage, the instantaneous shear modulus G and the initial shear stress τ_0 can be obtained from eq. (5) and eq. (6), respectively.

$$E_{fl} = Flex_i * E_i \tag{1}$$

$$\tau = G_0 \tan(\alpha) - \tau_0 : \alpha \leq \alpha_T. \tag{2}$$

$$\tau = G \tan(\alpha) + G_A - \tau_0 : \alpha > \alpha_T. \tag{3}$$

$$G_A = (G_0 - G)\tan(\alpha_T) \tag{4}$$

$$G = \frac{G_T}{1+tan^2(\alpha_T)} \tag{5}$$

$$\tau_0 = G_0 \tan(\alpha_0) \tag{6}$$

These equations define the constitutive response of the LAW58_FABR_A material model in Radioss, enabling the calibration of fiber tensile stiffness, shear modulus evolution, and the transition across the shear lock angle based on experimental data.

The LAW58 formulation accounts for the initial fiber stretch through parameters fitted from biaxial test data. When using uniaxial test data, the initial stretch parameters S_1 and S_2 were set to minimal residual values (1e-5) to avoid redundancy with the behavior already presented in the experimental curves. To record the results, a History Output was configured with a 0.05 s interval, measuring reaction forces at the reference nodes connected via couplings under enforced displacement. Simulation data were processed as in the experimental tests: stress was calculated as the reaction force divided by the cross-sectional area, and strain was computed from the displacement over time based on the imposed velocity and the initial gauge length.

Since only tensile tests were performed, the calibration process was conducted in two stages. First, the tensile curves at 0° and 90° were used to optimize the shear parameters. Subsequently, with the optimized shear data, a second optimization was performed using all parameterized values. Parameter calibration was carried out using the HyperStudy module, optimizing Radioss simulation results through the Global Response Search Method (GRSM). The GRSM is a deterministic, response-surface-based global optimization technique that builds and iteratively updates an adaptive response surface to explore the design space both locally and globally, generating a few designs per iteration and refining the model with new data, making it especially suitable for multi-objective problems or those with many design variables according to HyperStudy Help (2025) [9]. In this work, the objective function aimed to simultaneously minimize the area between the simulated and experimental curves in the warp, weft, and 45° diagonal directions, without assigning specific weights, thereby prioritizing a global fit of the material behavior.

Due to the material characteristics, the numerical solution was performed using an explicit solver. The continuous changes in the mechanical response, resulting from fiber elongation, require a time integration scheme that computes the next state directly from the current state using small time-steps. This contrasts with traditional implicit schemes, in which the future state is related to the current state through a global equation system, allowing larger time increments. In this case, the implicit approach would face severe convergence issues, as the input variables are time-dependent and undergo significant variation within a single time step. However, the use of explicit methods in long-duration simulations inherently leads to significantly higher computational times, as described by Hughes [10].

To enable calibration and optimization procedures, the total simulation time was reduced by increasing the displacement rate. To ensure numerical stability and computational efficiency, mass scaling was employed, a technique widely adopted in quasi-static analyses to prevent excessively small time-steps. In this study, the Advanced Mass Scaling (AMS) feature available in Radioss was used to increase the time increment without significantly altering the kinetic energy of the system. As inertial effects are negligible in quasi-static conditions, this approach is considered valid and is recommended by the Radioss Help (2021) [11].

3 Results

The experimental characterization of the Kairo Noir fabric served as the basis for the numerical calibration process. Initially, the quasi-static behavior of the system was assessed, confirming that variations in AMS did not influence the results. Following this verification, the shear behavior of the LAW58 material model was calibrated through a multi-objective optimization procedure in HyperStudy. This calibration enabled the accurate reproduction of the fabric's experimental stress–strain response in the three principal orientations: warp (0°), weft (90°), and diagonal (45°). Figure 5 presents the comparison between the simulated and experimental curves showing strong correlation, based on uniaxial test data after the first optimization of the LAW58 model. This consistency is confirmed by the coefficient of determination (R^2), which was equal to 1.0000 in the warp and weft directions and 0.9994 in the diagonal direction, indicating high fidelity in representing the orthotropic mechanical behavior of the fabric. The final parameters identified for the shear response of the fabric were an initial shear modulus $G_0 = 2.7991$ MPa, a shear locking angle $\alpha_T = 9.1055°$, and a tangent shear modulus $G_T = 30.1901$ MPa.

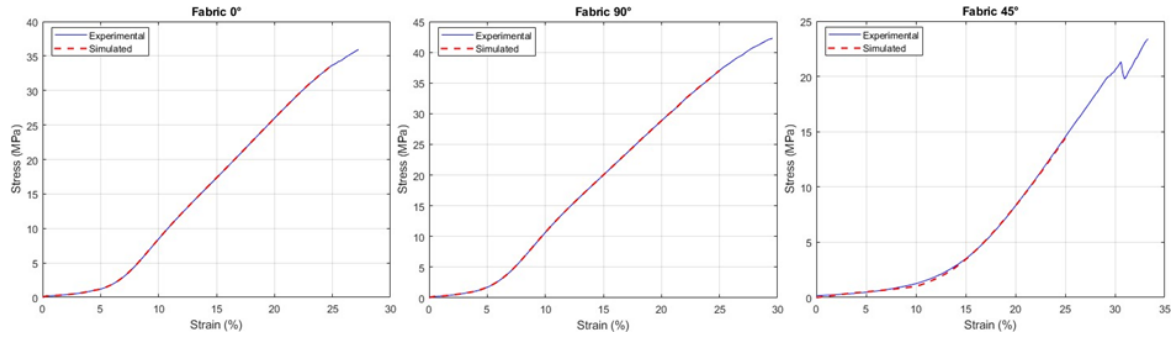


Figure 5 – First optimization of the LAW58 model based on uniaxial test data.

As the previously optimized shear parameters demonstrated stable performance in the simulations, a global optimization of all material parameters was subsequently conducted. The results of this optimization are presented in Fig. 6. This optimization was conducted solely using material parameters as input. The adopted values were: E_1 = 188.6543 MPa, E_2 = 175.1254 MPa, G_0 = 2.3734 MPa, G_T = 26.5501 MPa, α_T = 17.4530°, S_1 = 0.0477, S_2 = 0.0537, $Flex_1$ = 0.0094 and $Flex_2$ = 0.0126. The simulated stress-strain curves exhibited excellent agreement with the experimental data, with coefficients of determination (R^2) of 0.9984 in the warp direction (0°), 0.9968 in the diagonal direction (45°), and 0.9989 in the weft direction (90°), confirming that the calibrated model accurately captures the anisotropic mechanical behavior of the fabric.

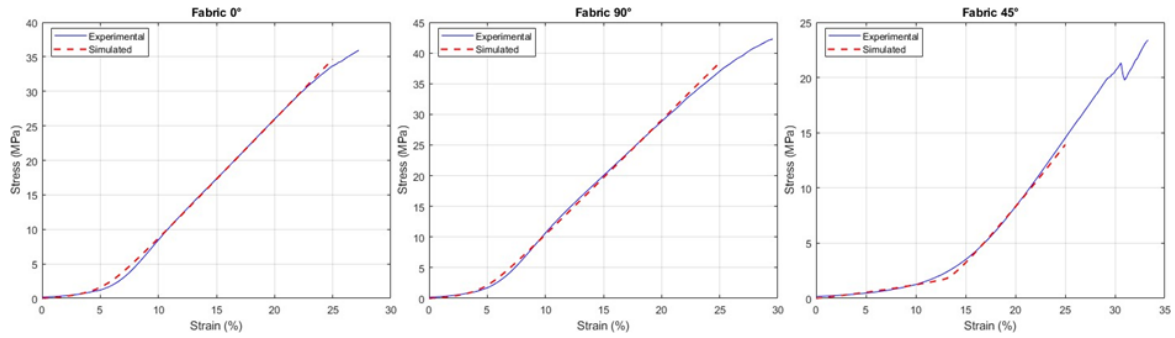


Figure 6 - Second optimization of the LAW58 model based on parametric input.

Although the first optimization resulted in better curve fitting, as indicated by higher R^2 values when compared to the second optimization, an analysis of the simulated deformation reveals an inconsistency. Specifically, the first set of parameters does not allow for observable deformation in the 0° and 90° directions, which does not reflect the actual fabric behavior. This discrepancy arises from the use of the uniaxial tensile test curve as input, along with very small straightening strain values in both directions (S_1 and S_2=1×10^{-5}). Such low values imply that the simulation assumes the fibers are already fully taut at the initial state, preventing realistic deformation. Ideally, a biaxial test curve should have been used as input for this parameterization. This behavior can be observed on Fig. 7.

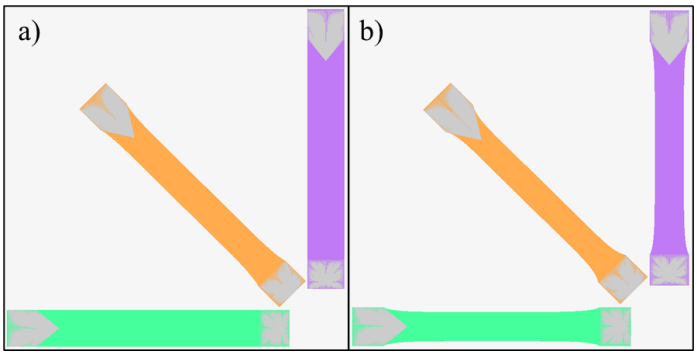


Figure 7 – Deformation patterns of the fabric model: (a) first optimization, (b) second optimization.

Despite the deformation inconsistency observed in the first optimization, it was used to define the initial shear parameters for the second optimization. This methodology allows fabric characterization using only uniaxial tensile tests at 0°, 45°, and 90°, unlike the conventional approach, which typically relies on biaxial and shear tests. These conventional tests are generally more complex and require specific equipment, whereas uniaxial tensile testing is simpler and more accessible. Thus, the proposed approach combining LAW58 with the AMS enables a viable material calibration, with LAW58 offering flexibility in the use of parameters and experimental curves, while the AMS significantly accelerates the numerical simulations, allowing a larger number of iterations for the optimization of the material parameters.

4 Conclusions

As a result of this study, the LAW58 material model in Radioss proved to be highly flexible as it allows the definition of material behavior either through experimental curves such as biaxial and shear tests or by directly specifying the parameters for the three principal material responses. Additionally, the use of AMS within the explicit solver is viable under certain conditions, such as quasi-static simulations, and can significantly enhance computational efficiency. This combination of material versatility and the solver's available resources enables a more adaptable and efficient calibration process, making optimal use of the available experimental data. In the present work, the calibration was performed in two stages: first, the tensile test curves at 0° and 90° were used to optimize the shear-related parameters; subsequently, a second optimization was carried out incorporating all material parameters.

Although the first optimization yielded good numerical agreement with the experimental curves, the simulated deformation pattern was not physically representative, specifically, no deformation occurred in the principal directions. This was attributed to the use of extremely small straightening strain values, which effectively constrained the initial deformation state. In the second optimization, with complete parameterization, it was possible to achieve both high correlation with experimental data and a physically consistent deformation response.

Therefore, the methodology presented in this work demonstrates that it is feasible to accurately characterize the orthotropic behavior of woven fabrics using only uniaxial tensile tests in the 0°, 45°, and 90° directions. This method eliminates the need for more complex tests, such as biaxial and shear testing, which require the use of specialized equipment to be performed, offering a practical and efficient alternative for material calibration.

Acknowledgements. The authors would like to express their gratitude to the Financiadora de Estudos e Projetos (FINEP) for their financial support of this project, under the contract code 01.24.0263.00.

Authorship statement. The authors hereby confirm that they are the sole liable persons responsible for the authorship of this work, and that all material that has been herein included as part of the present paper is either the property (and authorship) of the authors or has the permission of the owners to be included here.

References

[1] A. Hosseini, et al., "Identifying the distinct shear wrinkling behavior of woven composite preforms under bias extension and picture frame tests," Composite Structures, vol. 185, pp. 764–773, 2018.
[2] M. H. Kashani and A. S. Milani, "Damage prediction in woven and non-woven fabric composites," Non-woven Fabrics, pp. 233–262, 2016.
[3] É. P. das Neves et al., "Perception and fabrics: A preliminary investigation about the responses patterns by the stimulation of vision and touch," Design & Tecnologia, vol. 10, no. 20, pp. 95–105, 2020.
[4] X. Gao and L. Wang, "Finite element modelling for tensile behaviour of thermally bonded nonwoven fabric," AUTEX Research Journal, vol. 15, no. 1, pp. 48–54, Mar. 2015.
[5] A. Bydełek, M. Berdychowski, and K. Talaśka, "Modeling of material characteristics of conventional synthetic fabrics," AUTEX Research Journal, vol. 23, no. 2, pp. 200–208, 2023.
[6] Dassault Systèmes Simulia Corp., Abaqus User's Manual, Version 6.14, Section 23.4.1, Fabric material behavior, "FABRIC: Specify the in-plane response of a fabric material," 2014.
[7] International Organization for Standardization, ISO 13934-1:2013, "Textiles – Tensile properties of fabrics – Part 1: Determination of maximum force and elongation at maximum force using the strip method," 2013.
[8] Altair Engineering Inc., Radioss Help 2021 – /MAT/LAW58 (FABR_A). Available: https://2021.help.altair.com/2021/hwsolvers/rad/topics/solvers/rad/mat_law58_fabr_a_starter_r.htm
[9] Altair Engineering Inc., HyperStudy Help 2025 – Optimization Methods. Available: https://2025.help.altair.com/2025/hwdesktop/hst/topics/design_exploration/methods_optimization_r.htm
[10] T. J. R. Hughes, The Finite Element Method: Linear Static and Dynamic Finite Element Analysis. Mineola, NY, USA: Courier Corporation, 2003.
[11] Altair Engineering Inc., Advanced Mass Scaling (AMS) – Increase Computation Speed and Maintain Accuracy, in Radioss 2021 User's Guide: Capabilities and Limitations, Recommended Checklist, and Example Applications, 2021. Available: https://2021.help.altair.com/2021/hwsolvers/rad/topics/solvers/rad/advanced_mass_scaling_guidelines_c.htm